Journal of the Korean Nuclear Society
Volume 22, Number 2, June. 1990

Effectiveness of the Discrete Elements Method for the Slab-Geometry Neutron Transport Equation

Byung Chan Na and Jong Kyung Kim
Hanyang University
(Received February 14, 1990)

1차원 평판에서 Discrete Elements Method의 정확도에 대한 연구

나병찬 · 김종경
한양대학교
(1990. 2. 14접수)

Abstract

The new discrete elements method (DEM) is applied to the one-group neutron transport equation in one-dimensional slab geometry. The fixed source and the criticality problems are treated and three spatial differencing schemes (the DD, the SC, and the LC schemes) are tested to determine the most computationally efficient in the DEM.

In all cases, the accuracy of the results obtained from the DEM shows an improvement over that obtained from the standard discrete ordinates calculations. And the LC scheme gives the most accurate results in the DEM.

요 약

새로운 중성자 수송방정식의 해법인 Discrete Elements Method(DEM)를 1차원 모델에 대한 단일 에너지 중성자 수송방정식에 적용했다.

본 연구에서는 고정선원문제와 임계계산을 행하여, 각분할법과 DEM의 계산결과의 정확도를 비교했으며 세가지의 위치차등법(DD, SC 그리고 LC Scheme)중 어떤 것이 DEM에서 가장 좋은 지를 오차분석을 통해 정량적으로 알아 보았다. 수행한 모든 계산결과에서 같은 위치차등법을 이용할 때 DEM결과의 정확도가 각분할법으로 얻은 결과보다 훨씬 좋았으며 위치차등법중에서는 각분할법에서와 같이 DEM에서도 LC scheme이 가장 좋은 결과를 주었다.

I. Introduction

The discrete ordinates method (DOM) for obtaining numerical solutions to the integro-differential form of the transport equations has been used extensively in reactor calculations. In this method, a set of discrete directions for $\hat{\Omega}$ is chosen, and the transport equation is evaluated for these fixed directions. Each discrete direction can be visualized as a point on the surface of a unit sphere.

In more physical respects, the assumption underlying the neutron transport equation is that neutrons stream in straight lines between collisions

and that all directions of streaming are possible. In the DOM, only a few streaming directions are allowed. In effect, this restriction changes the basic physical model. This fact is the most important cause of the inaccuracy of the DOM and the ray effects in a two-or three-dimensional problem. So efforts to accurately solve the neutron transport equation have been sustained. That is, various angular quadrature sets[1,2] and higher order spatial schemes[3,4,5] have been developed. But the essential feature of the DOM which is the use of the fixed discrete directions is not altered.

To improve this limitation of the DOM, the discrete elements method (DEM) was proposed by K.A. Mathews in the early 1980s.[6] In the DEM, the angular variable of the neutron flux is discretized into a number of solid angle elements in a unit sphere, and the neutron transport equation is evaluated for these directions by suitable averaging processes. Therefore, within each solid angle element, the neutron streaming directions can be steered by changing physical conditions of a medium.

The element directions are determined by the appropriate numerical quadrature rule and the conventional DOM for each solid angle element. Evaluating the transport equation in the steered element directions is then done by using the spatial differencing scheme.

As a result of such a treatment of the angular variables, we can consider more accurate streaming directions of neutrons in the DEM than those in the DOM. Therefore we can strongly diminish the cause of the inaccuracy in the discrete ordinates results.

II. Theory

Let us consider the time-independent one-group transport equation in slab geometry[7]

$$\mu \frac{\partial}{\partial x}\Psi(x,\mu)+\Sigma_t(x)\Psi(x,\mu)=q(x,\mu), \tag{1}$$

where

$$q(x,\mu)=\int_{4\pi}\Sigma_s(x,\mu'\rightarrow\mu)\Psi(x,\mu')d\mu'+s(x,\mu). \tag{2}$$

The notation is conventional

By integrating Eq.(1) over the solid angle element domain μ_m, we obtain the discrete elements form of the one-group neutron transport equation

$$\frac{\partial}{\partial x}[\mu_m(x)\Psi_m(x)]+\Sigma t(x)\Psi_m(x)=q_m(x), \tag{3}$$

$m=1,2,\cdots, M$.

In Eq.(3), we have defined the average element angular flux $\Psi_m(x)$, element current $J_m(x)$, and element source $q_m(x)$ as

$$\Psi_m(x)\equiv\frac{1}{W_m}\int_{\mu m}\Psi(x,\mu)\,d\mu, \tag{4}$$

$$J_m(x)\equiv\frac{1}{W_m}\int_{\mu_m}\mu\Psi(x,\mu)\,d\mu, \tag{5}$$

$$q_m(x)\equiv\frac{1}{W_m}\int_{\mu m}q(x,\mu)\,d\mu, \tag{6}$$

with the element weight defined as

$$W_m\equiv\int_{\mu m}d\mu. \tag{7}$$

In addition, we have also defined the element direction (called" the flux weighted mean streaming direction") as

$$\mu_m(x)\equiv\frac{\int_{\mu m}\mu\Psi(x,\mu)\,d\mu}{\int_{\mu_m}\Psi(x,\mu)\,d\mu}. \tag{8}$$

where μm is the domain of angle of the m-th discrete angle element. If we obtain $\Psi_m(x)$ for all m by solving Eg.(3), the scalar flux can be determined as

$$\Phi(x)=\sum_{m=1}^{M}W_m\Psi_m(x). \tag{9}$$

To solve this set of M coupled differential equations [Eq.(3)], discretization of the spatial variables by applying finite difference techniques is required. To this end, various spatial differencing schemes have been developed. At present, there are three representative spatial differencing schemes(i.e., the DD, the SC, and the LC

schemes). When the spatial variable is discretized into the spatial grid with I mesh points, we assume that $\Sigma(x)=\Sigma_i$ and $\mu_m(x)=\mu_{mi}$ over a mesh cell i.

First, we introduce the Diamond Differencing (DD) scheme[3,4,5] (for $\mu_{mi}>0$)

$$\Psi_{mi+1/2}=\frac{2-\varepsilon_{mi}}{2+\varepsilon_{mi}}\Psi_{mi-1/2}+\frac{2}{2+\varepsilon_{mi}}\frac{q_{mi}}{\Sigma_{ti}} \tag{10}$$

where

$$\varepsilon_{mi}=\frac{\Sigma_{ti}\Delta x_i}{\mu_{mi}}. \tag{11}$$

It is observed that even if $\Psi_{mi-1/2}$ and q_{mi} are positive, Eq.(10) can give a negative value for $\Psi_{mi+1/2}$ if $\varepsilon_{mi}>2$. Therefore computer codes using the DD scheme include a negative-flux-fixup.

For another choice, we can use the following Step Characteristic (SC) scheme[3,4,5,8] (for $\mu_{mi}>0$):

$$\Psi_{mi+1/2}=\Psi_{mi-1/2}\exp(-\varepsilon_{mi})+\frac{q_{mi}}{\Sigma_{ti}}\left[1-\exp(-\varepsilon_{mi})\right] \tag{12}$$

and

$$\Psi_{mi}=\frac{q_{mi}}{\Sigma_{ti}}-\frac{1}{\varepsilon_{mi}}(\Psi_{mi+1/2}-\Psi_{mi-1/2}). \tag{13}$$

For positive values of $\Psi_{mi-1/2}$ and q_{mi}, we see that Eq.(12) does not give a negative value for $\Psi_{mi+1/2}$ and thus this scheme gives the positive flux.

Last, we have obtained the following Linear Characteristic(LC) scheme[3,4,5,9] (for $\mu_{mi}>0$):

$$\Psi_{mi+1/2}=\Psi_{mi-1/2}\exp(-\varepsilon_{mi})+\frac{q_{mi}}{\Sigma_{ti}}\left[1-\exp(-\varepsilon_{mi})\right] \tag{12}$$

$$+\frac{q_{mi+1/2}-q_{mi-1/2}}{\Sigma_{ti}}\times\left\{1-\left(\frac{1}{2}+\frac{1}{\varepsilon_{mi}}\right)\left[1-\exp(-\varepsilon_{mi})\right]\right\} \tag{14}$$

and

$$\Psi_{mi}=\frac{q_{mi}}{\Sigma_{ti}}-\frac{1}{\varepsilon_{mi}}(\Psi_{mi+1/2}-\Psi_{mi+1/2}). \tag{15}$$

This scheme always gives the positive flux.

In practice, we separate the $\mu_{mi}<0$ from the $\mu_{mi}>0$ directions in order to construct marching schemes that follow the direction of neutron streaming. If we note that boundary conditions are imposed on the incoming boundaries, it is apparent that we can advance the solution away from the incoming boundaries and in the direction of neutron streaming.

Next our concern is how we can determine the flux weighted mean streaming direction $\mu_m(x)$. It is achieved by integrating the integrals in Eq.(8). These integrals are approximated by the three-point Gauss-Legendre quadrature rule.[10] Of course, the choice of other quadrature rules is possible, but the Gauss-Legendre quadrature rule is the most simple and effective. In applying the Gauss-Legendre quadrature rule, it is necessary to have three fixed auxiliary directions and the corresponding auxiliary fluxes in each element. These are directly determined by the quadrature rule and the conventional discrete ordinates calculation.[11] (The same source term is used in calculations of both the DOM and the DEM.) Then, $\mu_m(x)$ can be expressed as

$$\mu_m(x)=\frac{w_m^u\mu_m^u\Psi_m^u(x)+w_m^c\mu_m^c\Psi_m^c(x)+w_m^d\mu_m^d\Psi_m^d(x)}{w_m^u\Psi_m^u(x)+w_m^c\Psi_m^c(x)+w_m^d\Psi_m^d(x)}, \tag{16}$$

where

$$w_m^u=5/9, \tag{17.a}$$

$$w_m^c=8/9, \tag{17.b}$$

$$w_m^d=5/9, \tag{17.c}$$

and

$$\mu_m^c=2(m-\frac{1}{2})/M \quad (m=1,2,\cdots,M/2), \tag{18.a}$$

$$\mu_m^u=\mu_m^c+\sqrt{0.6}/M, \tag{18.b}$$

$$\mu_m^d=\mu_m^c-\sqrt{0.6}/M, \tag{18.c}$$

where $M/2$ is the number of equal subintervals into which the interval $0<\mu<1$ is divided, and three fixed auxiliary directions in each angular element are labeled as up, center, and down, and $\Psi_m^c(x)$ represents $\Psi(x,\mu_m^c)$, and so on. And with this quadrature rule, the element weights are given by

$$w_m=2/M. \tag{19}$$

Then, using Eqs.(17.a) through (18.c), Eq.(16) for $\mu_m(x)$ becomes

$$\mu_m(x)=\mu_m^c+\frac{\sqrt{0.6}\ [\Psi^u(x)-\Psi^d(x)]}{M[\Psi^u(x)+1.6\Psi^c(x)+\Psi^d(x)]} \tag{20}$$

where all fluxes $\Psi(x)$ are obtained from the DOM.

We can see in Eq.(20) that $\mu_m(x)$ is a function of the position. That is, in each element and each cell, according to the auxiliary fluxes, the main streaming directions can be controlled. As a result, the direction of streaming of neutrons is accurately modeled.

In addition, the streaming direction as a function of the position results in the discontinuity at the interfaces of the spatial mesh cells. Therefore, for conservation of particles, the continuity of the current across cell interfaces is required. But within each mesh cell, conservation of particles is automatically preserved since the streaming directions were assumed to be constant within mesh cells. In the DOM, however, because the streaming directions are always fixed, the continuity of the flux across the cell interfaces is sufficient for conservation of particles.

III. Numerical Experiments and Discussions

The DEM described in the preceding section is implemented for the solution of two one-group transport problems in one-dimensional slab geometry. One is the fixed source problem. The other is the criticality calculation. The discrete elements solutions using three spatial differencing schemes are compared with those obtained from the DOM. Through an error analysis, it is shown that the DEM gives more accurate results than the DOM and the LC scheme is the most efficient spatial differencing scheme in the DEM.

1. Fixed Source Problem

We test the one-group isotropic scattering and source model problem in one-dimensional slab geometry. A total of forty spatial intervals, which are uniform within a 5 cm thick slab, is used in all test calculations. The total and scattering cross section are 2 cm^{-1} and 1 cm^{-1}, respectively. The isotropic external source strength is 2 neutrons/cm^2 sec and vacuum boundary conditions are imposed at both left and right boundaries. Three spatial differencing schemes are then tested and the pointwise convergence criterion is 10^{-5}. To evaluate the accuracy of each scheme in each method, we introduce the following error norm defined by

$$\| \Phi \| = \frac{| \sum_i (\Phi_i - \Phi_i^{bench}) |}{| \sum_i \Phi_i^{bench} |}, \quad i=1,2,\cdots,I. \tag{21}$$

Here, Φ^{bench} is the benchmark solution, while Φ is the calculated value.

Table 1 presents the error norms of the DOM and the DEM results for each spatial scheme, using the S_{32} results as the benchmark solutions. Table 2 shows the ratios of the error norm of the DEM to that of the DOM results for each scheme. And these results are plotted in Fig.1. In each spatial scheme, the DEM results converge to the

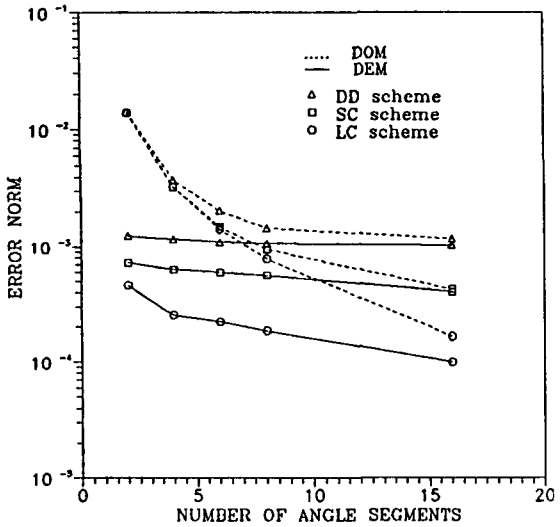

Fig.1 Error Norm vs. Number of Angle Segments in the Fixed Source Problem

benchmark solution faster than the equivalent DOM results. In particular, when the LC scheme is used, the most accurate results are obtained. When the calculations are performed in small M(number of angle segments), the superiority of the DEM is prominent. In the DEM, the values of the error norms of the DD or SC scheme are nearly constant with increasing M, that is, it approaches a certain asymptotic value. Because each spatial scheme itself has a certain order of the error for a given spatial mesh interval (The DD, the SC, and the LC schemes exhibit second-, second-, and fourth-order truncation error, respectively.), this asymptotic value is the minimal error with the DD or the SC scheme for forty mesh intervals. Therefore, the error can not be lessened below this value. In the DEM results, though M is only 2, the error is nearly the asymptotic value. And the DEM with the LC scheme gives the best results. Table 2 represents this fact clearly. When the same spatial scheme is used in the DOM and the DEM, the DEM gives more accurate results than the DOM, and when the LC scheme is used, the degree of that is eminent.

In addition, the computing time to solve the problem by the DEM takes four times than that of the DOM for the same M. But for small M, the DEM provides a solution more accurate than the DOM for a given computing time. That is, the DEM is more cost effective. But with increasing M, it becomes blunt, however the results are more accurate.

Table 1. Error Norms for Each Spatial Scheme in the DOM and the DEM

	DOM			DEM		
M[a]	DD	SC	LC	DD	SC	LC
2	0.01418	0.01396	0.01390	0.00124	0.00073	0.00046
4	0.00381	0.00328	0.00332	0.00116	0.00064	0.00026
6	0.00204	0.00149	0.00142	0.00109	0.00060	0.00022
8	0.00144	0.00094	0.00079	0.00107	0.00056	0.00019
16	0.00117	0.00043	0.00017	0.00103	0.00041	0.00009

a : Number of angle segments

Table 2. Ratio of the Error Norms in the DEM to the Error Norms in the DOM for Each Spatial Scheme

M	DD	SC	LC
2	0.087	0.052	0.033
4	0.304	0.194	0.077
6	0.535	0.405	0.157
8	0.741	0.595	0.236
16	0.877	0.952	0.602

2. Criticality Calculations

In order to check the accuracy of the DEM with another problem, the calculations are performed to determine the number of secondary neutrons per collision for criticality (called "c value" in general) for a given slab thickness "a". The cal-

Table 3. Number of Secondary Neutrons per Collision for Criticality in a Slab with 0.7366 mfp Half-Thickness

	Exact[a] : 1.40000					
	DOM			DEM		
M	DD	SC	LC	DD	SC	LC
2	1.53976 (9.984)[b]	1.53976 (9.983)	1.53967 (9.977)	1.40107 (0.077)	1.40112 (0.081)	1.40098 (0.070)
4	1.42799 (2.000)	1.42804 (2.003)	1.42792 (1.994)	1.40051 (0.037)	1.40063 (0.045)	1.40048 (0.034)
6	1.40891 (0.636)	1.40899 (0.642)	1.40885 (0.632)	1.40036 (0.026)	1.40048 (0.035)	1.40033 (0.024)
8	1.40402 (0.287)	1.40411 (0.294)	1.40396 (0.284)	1.40028 (0.020)	1.40041 (0.029)	1.40026 (0.019)
16	1.40087 (0.062)	1.40097 (0.068)	1.40083 (0.059)	1.40017 (0.013)	1.40031 (0.022)	1.40015 (0.011)
32	1.40027 (0.020)	1.40038 (0.028)	1.40023 (0.017)	1.40012 (0.009)	1.40025 (0.018)	1.40009 (0.007)

a : Refer to Ref.(12)

b : Relative errors in percent

culations are made for slabs with the half thickness of 0.7366, 1.2893, and 5.6655 mean free paths and a total of forty spatial intervals is used. (Three slab thicknesses will be designated as case 1,2, and 3, respectively.) Also, three spatial schemes are tested and the pointwise convergence criterion is 10^{-5}.

For each iteration the c value is evaluated from the neutron conservation principle :

$$c=1+2\frac{\int_{-1}^{1}\mu\Psi(\frac{a}{2},\mu)d\mu}{\int_{-\frac{a}{2}}^{\frac{a}{2}}dx\int_{-1}^{1}\Psi(x,\mu)d\mu} \quad (22)$$

The spatial integration may be performed by using Simpson's rule.[10]

In Table 3 through 5, the results are shown for the criticality calculations carried out in the slab with three different thicknesses. All of these results

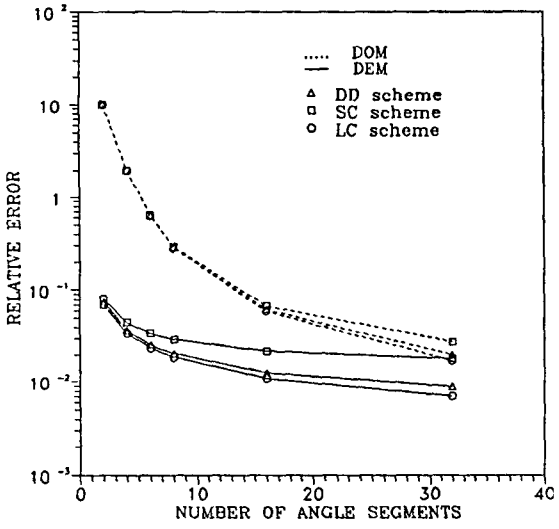

Fig.2 Relative Error vs. Number of Angle Segments for 0.7366 mfp Half-thick Slab in the Criticality Calculation

are plotted in Fig.2 through 4. In all cases, the accuracy of the DEM results is superior to that of the DOM. It is observed that the SC scheme is less accurate than any other schemes. This is because the SC scheme overestimates the flux at the slab boundaries. That is, the leakage at this position [see Eq.(22)] is greater than a real value. In case 1, as shown in Table 3/Fig.2, the DEM is cost effective. In cases 2 and 3 for thicker slab, with increasing M, the accuracy of the DOM is

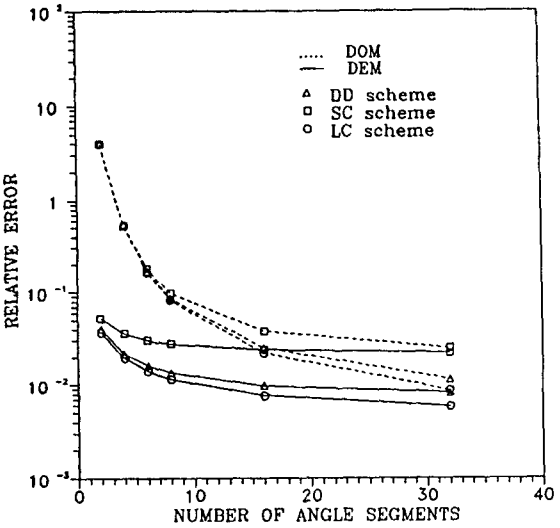

Fig.3 Relative Error vs. Number of Angle Segments for 1.2893 mfp Half-thick Slab in the Criticality Calculation

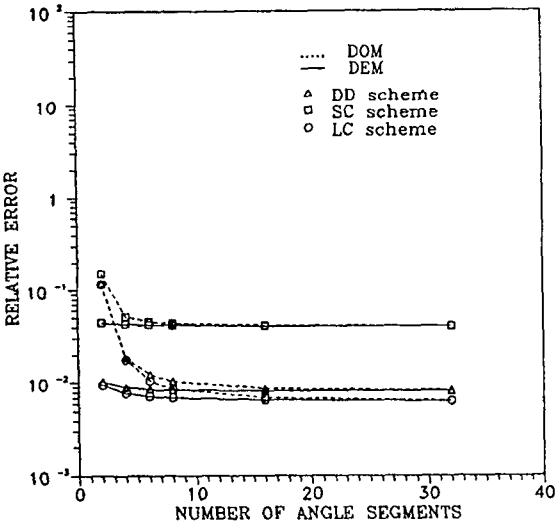

Fig.4 Relative Error vs. Number of Angle Segments for 5.6655 mfp Half-thick Slab in the Criticality Calculation

comparable to that of the DEM. Of course, even these cases, the DEM results are more accurate than the DOM results when the same spatial scheme is used in both methods.

IV. Conclusions

The main conclusions that can be drawn from our work are as follows :

1. The discrete elements equations, combined with any spatial differencing schemes, produce a set of equations that can be easily solved by using the computer with the same iterative procedures used in the conventional discrete ordinates method.

2. For fixed source problem, the DEM supplies a solution more accurate than the DOM, Specially, when the DEM is combined with the LC scheme, this advantage is remarkable. With small M, the performance of the DEM is better than the DOM for a given computing time. However, by increasing M, the computing times required by the DEM may be greater than those by the DOM, but the results are more accurate.

3. For criticality calculations, the DEM works better than the DOM. This is particularly prominent in a thin slab. The SC scheme gives much less accurate results than the DD scheme because of the overestimation at the slab boundaries. The DEM with the LC scheme gives the most accurate results.

In the present work, the DEM is applied to only the one-group transport problems with isotropic scattering and sources. Several possibilities still exist for the extension of the present work to more general physical situations given as follows :

1. It is possible that the extension of the DEM to other geometries.

Table 4. Number of Secondary Neutrons per Collision for Criticality in a Slab with 1.2893 mfp Half-Thickness

Exact[a] : 1.20000						
	DOM			DEM		
M	DD	SC	LC	DD	SC	LC
2	1.24700 (3.917)[b]	1.24708 (3.924)	1.24693 (3.911)	1.20048 (0.040)	1.20063 (0.053)	1.20043 (0.037)
4	1.20631 (0.526)	1.20644 (0.537)	1.20626 (0.522)	1.20025 (0.022)	1.20042 (0.036)	1.20023 (0.019)
6	1.20200 (0.167)	1.20214 (0.179)	1.20196 (0.163)	1.20019 (0.016)	1.20036 (0.030)	1.20016 (0.014)
8	1.20103 (0.086)	1.20118 (0.099)	1.20099 (0.083)	1.20016 (0.014)	1.20033 (0.028)	1.20013 (0.011)
16	1.20029 (0.025)	1.20045 (0.038)	1.20026 (0.022)	1.20011 (0.010)	1.20028 (0.024)	1.20009 (0.008)
32	1.20013 (0.011)	1.20029 (0.025)	1.20010 (0.009)	1.20009 (0.008)	1.20026 (0.022)	1.20007 (0.006)

a : Refer to Ref.(12)

b : Relative errors in percent

Table 5. Number of Secondary Neutrons per Collision for Criticality in a Slab with 5.6655 mfp Half-Thickness

Exact[a] : 1.02000						
	DOM			DEM		
M	DD	SC	LC	DD	SC	LC
2	1.02119 (0.118)[b]	1.02154 (0.151)	1.02118 (0.116)	1.02010 (0.010)	1.02045 (0.045)	1.02009 (0.010)
4	1.02018 (0.019)	1.02053 (0.052)	1.02018 (0.018)	1.02009 (0.009)	1.02043 (0.042)	1.02998 (0.008)
6	1.02012 (0.012)	1.02046 (0.046)	1.02010 (0.011)	1.02008 (0.008)	1.02042 (0.042)	1.20007 (0.007)
8	1.02010 (0.010)	1.02044 (0.044)	1.02008 (0.009)	1.02008 (0.008)	1.02042 (0.042)	1.02007 (0.007)
16	1.02008 (0.009)	1.02042 (0.042)	1.02007 (0.007)	1.02008 (0.008)	1.02041 (0.041)	1.20006 (0.007)
32	1.02008 (0.008)	1.02041 (0.041)	1.02006 (0.006)	1.02008 (0.008)	1.02041 (0.040)	1.02006 (0.006)

a : Refer to Ref.(12)

b : Relative errors in percent

2. The inclusion of the DEM into a more general mulatigroup formalism would be a useful extension of the present study.

3. A third would be the inclusion of anisotropic scattering. Including linear anisotropy in this work is straightforward.

References

1. K.D. Lathrop and B.G. Carlson, "Discrete Ordinates Angular Quadrature of the Neutron Transport Equation," LA-3186, Los Alamos Scientific Laboratory, February 1965.
2. I.K. Abu-Shumays, "Compatible Product Angular Quadrature for Neutron Transport in X-Y Geometry," *Nucl. Sci. Eng.*, **61,** 299(1977).
3. R.E. Alcouffe, et al., "Computational Efficiency of Numerical Methods for the Multigroup, Discrete–Ordinates Neutron Transport Equations : The Slab Geometry Case," *Nucl. Sci. Eng.*, **71,** 111(1979).
4. E.W. Larsen and W.F. Miller, Jr., "Convergence Rates of Spatial Difference Equations for the Discrete–Ordinates Neutron Transport Equations in Slab Geometry," *Nucl. Sci. Eng.*, **73,** 76(1980).
5. S.M. Lee and R. Vaidyanathan, "Comparison of the Order of Approximation in Several Spatial Difference Schemes for the Discrete–Ordinates Transport Equation in One–Dimensional Plane Geometry," *Nucl. Sci. Eng.*, **76,** 1(1980).
6. K.A. Mathews, "Discrete Elements Method of Neutron Transport," *Nucl. Sci. Eng.*, **98,** 41(1988).
7. J.J. Duderstadt and W.R. Martin, "Transport Theory," Chap.1, John Wiley & Sons, New York, 1979.
8. K.D. Lathrop, "Spatial Differencing of the Transport Equation : Positivity vs. Accuracy," *J. Comput. Phys.*, **4,** 475(1969).
9. D.V. Gopinath, A. Natarajan, and V. Sundararaman, "Improved Interpolation Schemes in Anisotropic Source Flux Iteration Techniques," *Nucl. Sci. Eng.*, **75,** 181(1980).
10. S.S. Kuo, "Computer Applications of Numerical Methods," Chap.12, Addition-Wesley Publishing Company, Massachusetts, 1972.
11. R.D. O'Dell and R.E. Alcouffe, "Transport Calculations for Nuclear Analyses : Theory and Guidelines for Effective Use of Transport Codes," LA–10983–MS, Los Alamos National Laboratory, September 1987.
12. H.G. Kaper, A.J. Lindeman, and G.K. Leaf, "Benchmark Values for the Slab and Sphere Criticality Problem in One–Group Neutron Transport Theory," *Nucl. Sci. Eng.*, **54,** 94(1974).